Clay Minerals, (2017) **52**, 485–496

Alkali activation of natural clay using a $Ca(OH)_2/Na_2CO_3$ alkaline mixture

F. SHAQOUR[1], M. ISMEIK[2,3] AND M. ESAIFAN[4,*]

[1] *Department of Applied Geology and Environment, The University of Jordan, Amman 11942, Jordan*
[2] *Department of Civil Engineering, The University of Jordan, Amman 11942, Jordan*
[3] *Department of Civil Engineering, Australian College of Kuwait, Safat 13015, Kuwait*
[4] *Department of Chemistry, The University of Jordan, Amman 11942, Jordan*

(*Received 23 July 2017; revised 19 December 2017; Associate Editor: Joao Labrincha*)

ABSTRACT: An experimental investigation was conducted on the alkali activation of a kaolinitic clay using an alkaline mixture composed of hydrated lime ($Ca(OH)_2$) and sodium carbonate (Na_2CO_3) solution. The $Ca(OH)_2/Na_2CO_3$ alkaline mixture was developed to overcome the high cost and chemical aggression associated with classical alkaline solutions. The mineralogical composition and microstructure of the alkaline mixture and alkali-activation products were studied using X-ray diffraction, attenuated total reflectance-Fourier transform infrared spectroscopy, thermogravimetric analysis and energy-dispersive X-ray-scanning electron microscopy techniques. Pirssonite ($Na_2Ca(CO_3)_2{\cdot}2H_2O$), calcite ($CaCO_3$), and sodium hydroxide (NaOH) formed as a result of mixing of $Ca(OH)_2$ with Na_2CO_3. The alkali activation of natural clay with the $Ca(OH)_2/Na_2CO_3$ alkaline mixture produced a binding agent identified as hydroxysodalite phase ($Na_8Al_6Si_6O_{24}(OH)_2{\cdot}4H_2O$) when pure kaolinite was used, and cancrinite carbonate ($Na_6Ca_{1.5}[Al_6Si_6O_{24}](CO_3)_{1.5}{\cdot}1.8H_2O$) when kaolinitic clay with high a calcite content was used. The mechanical strength of the binder developed was evaluated on cylindrical specimens containing granite waste as a filler material under dry and soaked conditions. The classical NaOH activator was used for comparison. For specimens produced using a $Ca(OH)_2/Na_2CO_3$ mixture as the alkaline activator, the recorded strength value was 21 MPa which was 35% less than that achieved by the classical NaOH solution. Durability tests on samples soaked in water for 24 h showed a reduction in strength from 34 to 22 MPa for specimens prepared with NaOH solution, and from 21 to 11 MPa for the specimens prepared with a $Ca(OH)_2/Na_2CO_3$ alkaline mixture.

KEYWORDS: kaolinitic clay, strength, alkali activation, $Ca(OH)_2$, Na_2CO_3, pirssonite, hydroxysodalite, cancrinite.

Alkali activation of aluminosilicates is a term used to describe synthesis of geopolymers, inorganic polymers or alkali-activated binders in a high-pH environment at relatively low curing temperatures, up to 100°C (Davidovits, 1991; Carvalho *et al.*, 2008; Provis & Bernal, 2014; Esaifan *et al.*, 2015). The mechanical strength (>40 MPa) of the alkali-activated materials with low-energy requirements during production, encouraged extensive research worldwide to use the alkali-activated materials as environmentally friendly alternative building materials to Portland cement (Carvalho *et al.*, 2008; Van Deventer *et al.*, 2012; Provis & Bernal, 2014; Esaifan *et al.*, 2016). The mechanical strength, morphology and physical properties of alkali-activated materials are influenced by several factors such as curing temperature, curing time, and type and concentration of the alkaline activator (Pacheco-Torgal *et al.*, 2014). The alkali activation of natural kaolinite using NaOH commonly produces hydrosodalite (Esaifan *et al.*, 2015; Maia *et al.*, 2015) or A-type and X-type zeolites (Belviso *et al.*, 2015; Menezes *et al.*,

* E-mail: mu.esaifan@ju.edu.jo
https://doi.org/10.1180/claymin.2017.052.4.06

2017). On the other hand, the use of a potassium hydroxide (KOH) solution yields a semi-crystalline potassium aluminosilicate phase ($KAlSiO_4$) identified as kaliophilite (Esaifan *et al.*, 2016). The reaction mechanism of the alkali-activation process has been summarized in three steps: (1) dissolution of aluminosilicate material into different monomeric species due to the high-pH environment; (2) restructuring or orientation of these mobile monomeric species to obtain a more thermodynamically stable state; and (3) polycondensation or precipitation of new hydrated aluminosilicate phases (Pacheco-Torgal *et al.*, 2008; Zhang *et al.*, 2008; Burciaga-Díaz & Escalante-García, 2013).

The major obstacles to commercializing the alkali-activated materials are the chemical aggression and costs associated with classical alkaline activators such as NaOH, KOH and alkali-silicate solution. Moderately alkaline reactants such as $Ca(OH)_2$, K_2CO_3 and Na_2CO_3 have been investigated in terms of producing alkali-activated materials. However, the use of these activators as a single reactant provided a poor dissolution rate and mechanical strength properties in comparison with NaOH and KOH solutions (Gogo, 1990; Steudel *et al.*, 2013). Gogo (1990) studied the stabilization of soil using $Ca(OH)_2$ and K_2CO_3 as single additives or as a mixture. The application of these reactants in mixtures yielded greater mechanical strength than that obtained when these reactants were used as a single additive. Gogo (1990) proposed the formation of an intermediate phase of double carbonate from the $Ca(OH)_2/K_2CO_3/H_2O$ system as illustrated in equations 1 and 2. Steudel *et al.* (2013) also studied the use of Na_2CO_3 as a single alkaline activator for bentonite. They observed a limitation in the dissolution process due to the formation of double salts Ca^{2+}-Na^+ and precipitation of $CaCO_3$. In the work of Esaifan *et al.* (2016), the reaction products and stability of a $Ca(OH)_2/K_2CO_3/H_2O$ system were studied using a different storage time. That study yielded a double carbonate identified as butschliite ($Ca_2K_6(CO_3)_5{\cdot}6H_2O$) as well as KOH. The alkali-activated material of the kaolinitic clay using the $Ca(OH)_2/K_2CO_3/H_2O$ system was identified by Esaifan *et al.* (2016) as a hydrous phase of kaliophilite ($K_2Si_2Al_2O_8{\cdot}3H_2O$). In addition, for better mechanical-strength results, the $Ca(OH)_2$ powder should be mixed first with kaolinitic clay and then K_2CO_3 solution should be added to the mixture.

$$K_2CO_3 + Ca(OH)_2 \rightarrow 2KOH + CaCO_3 \quad (1)$$

$$8KOH + 6H_2O + 6CaCO_3 \rightarrow 4Ca(OH)_2 + Ca_2K_6(CO_3)_5 \cdot 6H_2O + K_2CO_3 \quad (2)$$

Kaolinite ($Al_2Si_2O_5(OH)_4$) or its thermally treated phase (metakaolinite) is the most widely used aluminosilicate material in the alkali-activation synthesis, due to its homogeneity, wide availability and unique structure that leads to high chemical reactivity (Osornio-Rubio *et al.*, 2016). The structure of kaolinite consists of alternating sheets of SiO_4 tetrahedra and Al octahedra joined by apical oxygen atoms. Kaolins are widely distributed in southern Jordan which makes them good precursors for the production of alkali-activated binders. Details of the kaolin reserves and their nature, character and economic importance were given by Khoury & El-Sakka (1986).

The current study investigated the possibility of using a mixture of $Ca(OH)_2$ and Na_2CO_3, as a low-cost alkaline activator with minimal chemical aggression to produce alkali-activated material. The chemical composition and microstructure of both the alkaline mixture and alkali-activated material were studied. Unconfined compressive strength testing was performed under dry and soaked conditions to evaluate the dimensional stability of the alkali-activated material produced.

EXPERIMENTAL

The kaolinitic clay was collected from the El-Hiswa deposit (coded as JHK-clay), which is located in southern Jordan. The clay was crushed and homogenized using a cone crusher (TRIO model TC36) equipped with micro-filters to obtain a particle size mostly <20 μm. The plastic limit was determined to be 28% according to ASTM standard D4318-10 (2017). Standard clay (coded as SK-clay) supplied by Merck KGaA (Germany) was used as a reference kaolinite material. Waste granite (WG-granite) collected from granite quarries in Jordan was used as a filler material. Filler materials are commonly used in alkali-activation synthesis to improve mixing workability, to reduce drying cracks caused by drying shrinkage and to reduce the production cost without loss of strength by reducing the amount of alkali-activated binder required in the final concrete matrix (Esaifan *et al.*, 2016). 100 kg of granite was crushed and sieved to obtain a particle size range of ≤450 μm. The chemical compositions of the clay samples and of the waste granite, as determined by X-ray fluorescence (XRF), are listed in Table 1. The Si/Al molar ratio values calculated are 2.8, 1.4 and 6.0 for the JHK-clay, SK-clay and WG-granite samples respectively. Alkaline reactants of analytical grade were supplied by Merck (Darmstadt, Germany) including $Ca(OH)_2$ (≥96.0%), NaOH (≥98.0%) and Na_2CO_3 (≥99.9%). The alkaline-

https://doi.org/10.1180/claymin.2017.052.4.06 Published online by Cambridge University Press

TABLE 1. Chemical analysis (wt.%) of JHK-clay, SK-clay and waste granite (WG).

Sample	SiO_2	TiO_2	Al_2O_3	TiO_2	MgO	CaO	Na_2O	K_2O	SO_3	LOI	Total	Si/Al ratio
JHK	52.4	0.5	19.2	0.5	0.3	6.7	0.5	3.7	0.2	7.4	99.7	2.8
SK	47.8	1.2	36.1	1.2	0.2	0.1	0.3	1.4	–	11.6	99.5	1.4
WG	69.5	0.5	12.1	0.5	0.3	3.2	3.5	2.7	0.4	0.7	99.8	6.0

LOI: Loss on ignition at 1000°C.

activating solutions were prepared using deionized Millipore water and used immediately.

In this study, the specimens were prepared using the mass ratios described by Esaifan *et al.* (2016). The mixing components of alkali-activated material were identified by the mass ratios of (granite/clay):(alkaline reactants/clay):(water/clay), where clay mass was considered as a reference and fixed at 100. The experimental work was divided into three steps. In the first step (1), the mineralogical composition of the alkaline mixture developed was studied at $Ca(OH)_2$ (8.0 M) and Na_2CO_3 (8.0 M) concentrations which is assumed to produce a NaOH solution with a theoretical maximum concentration of 15.8 M according to the reaction stoichiometry described in equation 3. This concentration of NaOH (15.8 M) is equivalent to the composition that is used to fabricate alkali-activated material with mass ratios of NaOH/clay, granite/clay and H_2O/clay equal to 0.16, 1 and 0.25, respectively. The alkaline mixture was mixed for 15 min using a magnetic stirrer, cured for 24 h at 70°C, crushed and finally characterized using powder X-ray diffraction (XRD) and thermogravimetric analysis (TGA). In step 2, the mineralogical compositions and microstructure of $Ca(OH)_2/Na_2CO_3$-based alkali-activated materials were studied in specimens prepared using JHK-clay and SK-clay for comparison. The mass ratios of $Ca(OH)_2$/clay and Na_2CO_3/clay were selected according to the stoichiometric ratio as described by equation 3 and assumed to produce NaOH with NaOH/clay mass ratios equivalent to 0.16 and 0.32 as listed in Table 2. The mixing process in this phase was performed using an IKA digital dual-range mixer (model IKA-RW20) at 300 rpm. After mixing, the specimens were dried in an oven at 70°C for 24 h, crushed, sieved (≤75 μm) and, finally, were characterized using XRD, TGA, attenuated total reflectance Fourier transform infrared (ATR-FTIR) spectroscopy and scanning electron microscopy (SEM).

In step 3, the dimensional stability of JHK-clay-based alkali-activated material under dry and soaked conditions was evaluated with the addition of granite (WG-granite) as filler material. Two sets of cylindrical specimens were fabricated (25 mm in diameter, 50–60 mm in height); the first set of specimens was prepared using a $Ca(OH)_2/Na_2CO_3$ alkaline mixture with mass ratios assumed to produce NaOH with NaOH/clay mass ratios of 0.10, 0.12, 0.14, 0.16 and 0.18, whereas mass ratios of granite/clay and water/clay were fixed at 1 and 0.25, respectively (Table 3). The second set of specimens was prepared using NaOH (reference alkaline activator) with NaOH/clay mass ratio similar to that produced using the $Ca(OH)_2/Na_2CO_3$ alkaline mixture (Table 3). The mixing was performed using a Hobart planetary mixer (model A200) at 198 rpm for a total period of 15 min. In the $Ca(OH)_2/Na_2CO_3$-based alkali-activated material,

TABLE 2. Mixed compositions of batches prepared for mineralogical and microstructure studies (phase II).

		Mass ratio (wt./wt.)		
Batch code	Clay sample	$Ca(OH)_2$/clay	Na_2CO_3/clay	Water/clay
Mix 1	JHK	0.16	0.23	0.25
Mix 2	JHK	0.36	0.52	0.25
Mix 3	SK	0.16	0.23	0.25
Mix 4	SK	0.36	0.52	0.25

https://doi.org/10.1180/claymin.2017.052.4.06 Published online by Cambridge University Press

TABLE 3. Mixed compositions of batches prepared for the dimensional stability study (phase III).

Batch Code	Mass ratio (wt./wt.)				
	Granite/clay	$Ca(OH)_2$/clay	Na_2CO_3/clay	NaOH/clay	Water/clay
Mix 5	1.00	0.10	0.14	–	0.25
Mix 6	1.00	0.12	0.17	–	0.25
Mix 7	1.00	0.14	0.20	–	0.25
Mix 8	1.00	0.16	0.23	–	0.25
Mix 9	1.00	0.18	0.27	–	0.25
Mix 10	1.00	–	–	0.10	0.25
Mix 11	1.00	–	–	0.12	0.25
Mix 12	1.00	–	–	0.14	0.25
Mix 13	1.00	–	–	0.16	0.25
Mix 14	1.00	–	–	0.18	0.25

$Ca(OH)_2$ powder was mixed first with clay and granite for 5 min then Na_2CO_3 solution was added and mixed with the final mixture for 10 min. The mixture was divided into six specimens (of ~50 g each) and moulded immediately in a stainless steel cylinder (25 mm internal diameter, 150 mm height) with a plunger and hydraulic press at a pressure of 15 MPa. The demoulded specimens were cured for 24 h at 70°C in a ventilated oven. Thereafter, the samples were removed, allowed to cool at room temperature and then divided into two groups of three specimens each. The first three specimens were tested under dry conditions, while the other three specimens were soaked in water for seven days prior to testing. The final strength values were reported as the average of three measurements.

The chemical compositions of JHK-clay and WG-granite was performed on fused pellets using a Shimadzu Lab Center XRF-1800 sequential X-ray fluorescence spectrometer (XRF) equipped with Rh anode X-ray tube with a maximum power of 3.8 kW. The mineralogical compositions and microstructure of the alkaline mixture and alkali-activated material were investigated by XRD, using a Shimadzu MAXima X XRD-7000 diffractometer with Cu-$K\alpha$ radiation (λ = 1.54 Å), 40 kV, 40 mA over a range of 2–70°2θ with a scan rate of 2°2θ/min, scanning step = 0.02° and receiving slit = 0.3 mm. The ATR-IR spectroscopy was used because of its ability to obtain IR spectra directly without preparation of KBr disks and destruction of the sample (Billingham *et al.*, 1996). A Thermo Scientific Nicolet spectrometer (IS50R) was used coupled with an ATR diamond crystal unit (Thermo Scientific Smart iTR). Spectra were collected from 4000 to 650 cm^{-1} at a resolution of 2 cm^{-1} and averaged over 32 scans. The thermal stability and dehydration of the Na_2CO_3/$Ca(OH)_2$ alkaline mixture and the alkali-activated materials produced were investigated by thermo-gravimetric analysis (TGA), using a NETZSCH (STA 409 PG/PC) thermal analyzer. About 35 mg was heated from 50 to 1000°C at 10°C min^{-1} under nitrogen gas atmosphere. The morphology of the alkali-activated materials was investigated by SEM (FEI Inspect, F50/FEG) coupled with a Bruker AXS EDS system. The SEM images were collected at 6.10^{-4} Pa with 30 kV accelerating voltage. The SEM imaging was conducted on platinum-coated specimens using a Quorum-Emitech K550X sputter coater. Unconfined compressive strength tests were conducted to evaluate the dimensional stability of Na_2CO_3/$Ca(OH)_2$-based alkali-activated material and NaOH-based alkali-activated material. The strength test was performed using a universal unconfined compression test machine with a strain rate of 1 mm/min.

RESULTS AND DISCUSSION

Study of the $Ca(OH)_2$/Na_2CO_3 alkaline mixture

The XRD pattern of a $Ca(OH)_2$/Na_2CO_3 alkaline mixture is presented in Fig. 1. The pattern contains $Ca(OH)_2$,Na_2CO_3 and a double Na-Ca carbonate identified as pirssonite ($Na_2Ca(CO_3)_2{\cdot}2H_2O$). In nature, double Na-Ca carbonates occur as two intermediate phases namely nyerereite ($Na_2Ca(CO_3)_2$) and shortite ($Na_2Ca_2(CO_3)_3$) (Boettcher & Gehlken, 1996; Shatskiy *et al.*, 2015). In previous

https://doi.org/10.1180/claymin.2017.052.4.06 Published online by Cambridge University Press

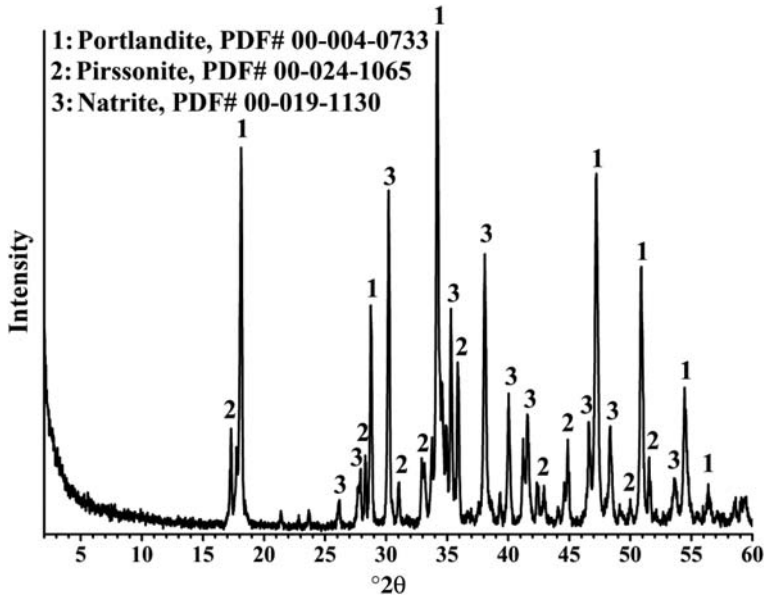

FIG. 1. XRD pattern of the $Ca(OH)_2/Na_2CO_3$ alkaline mixture developed.

works the synthesis of double Na-Ca carbonates was achieved at high temperature in hydrothermal experiments at 1 kbar and 450°C (Gavryushkin *et al.*, 2016), and in thermally induced solid-state reactions at temperatures >300°C (Smith *et al.*, 1971). No evidence for the presence of calcite ($CaCO_3$) was observed although it was expected from equation 3, which suggests a consecutive reaction between NaOH and $CaCO_3$ (equation 3 products) to produce $Ca(OH)_2$, Na_2CO_3 and pirssonite as described in equation 4.

$$Na_2CO_3 + Ca(OH)_2 \rightarrow 2NaOH + CaCO_3 \quad (3)$$

$$4CaCO_3 + 6NaOH + 2H_2O \rightarrow 3Ca(OH)_2 + 2Na_2CO_3 + Na_2Ca(CO_3)_2 \cdot 2H_2O \quad (4)$$

The thermal stability of the alkaline mixture developed was studied using TGA (Fig. 2). The alkaline mixture developed displays three stages of decomposition: stage I represents the decomposition of Na_2CO_3 and consists of two sharp endothermic peaks in the temperature range 20–255°C, with maxima at ~95°C and 168°C. Stage II represents the dehydration of $Ca(OH)_2$ and is reflected by a sharp endothermic peak in the range 290–500°C, with maximum at ~430°C. Stage III shows a more complicated decomposition process as reflected by two overlapping broad endothermic peaks, beginning at 510°C, and achieving maxima at ~725°C and 850°C. According to the XRD results, the third phase is attributed to the decomposition of pirssonite ($Na_2Ca(CO_3)_2 \cdot 2H_2O$).

Study of the $Ca(OH)_2/Na_2CO_3$-based alkali-activated material

The powder XRD patterns of SK-clay and its alkali-activated materials are shown in Fig. 3. The SK-clay consists almost exclusively of kaolinite (Fig. 3a). The dissolution of kaolinite using the alkaline mixture developed was confirmed by a remarkable decrease in the intensity of characteristic kaolinite reflections (12.3 and 24.9°2θ) with increasing mass ratios of $Ca(OH)_2$ and Na_2CO_3 (Fig. 3b,c). The dissolution of kaolinite was followed by the formation of a new phase indicated as hydroxysodalite with the main characteristic reflections at 14.1 and 24.5°2θ. The formation of hydroxysodalite by NaOH alkali activation of calcined or untreated clay was reported previously (Novembre *et al.,* 2011; Esaifan *et al.,* 2015). The release of NaOH from the $Ca(OH)_2/Na_2CO_3$ alkaline mixture was assumed from the formation of hydroxysodalite and calcite (cf. equation 3). Unlike the alkaline mixture, no evidential diffraction peaks were observed for pirssonite, suggesting that in the kaolinite/NaOH/$CaCO_3$ system, NaOH reacts first with kaolinite due to its high chemical reactivity compared to the $CaCO_3$ precipitated.

https://doi.org/10.1180/claymin.2017.052.4.06 Published online by Cambridge University Press

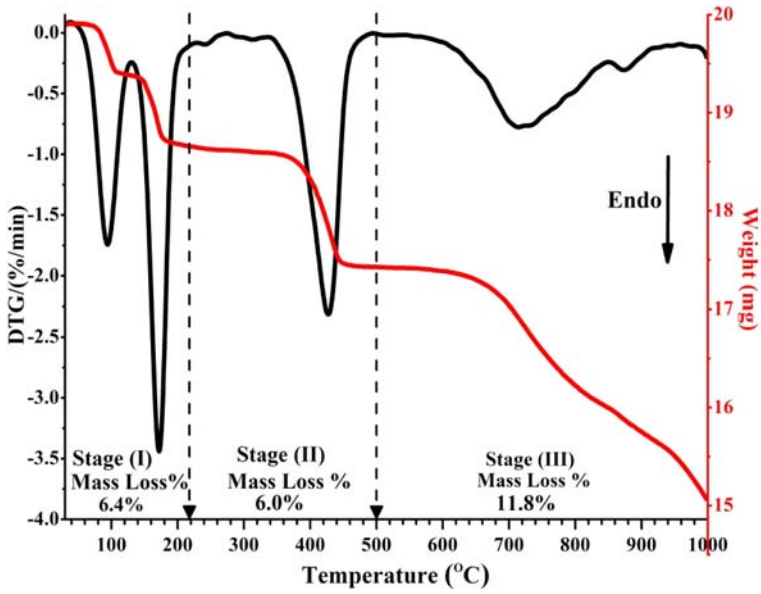

FIG. 2. TGA/DTG curves of the $Ca(OH)_2/Na_2CO_3$ alkaline mixture developed.

The powder XRD patterns of JHK-clay, and its alkali-activated material are shown in Fig. 4. The JHK-clay consists of kaolinite, quartz and calcite as major components and muscovite as a minor component (Fig. 4a). The alkali activation of JHK-clay with the alkaline mixture developed, yielded a cancrinite carbonate phase ($Na_6Ca_{1.5}[Al_6Si_6O_{24}](CO_3)_{1.5}\cdot 1.8H_2O$). Cancrinite carbonate is a porous aluminosilicate mineral with cage structure similar to that found in many zeolites (*i.e.* Hassan *et al.*, 2006).

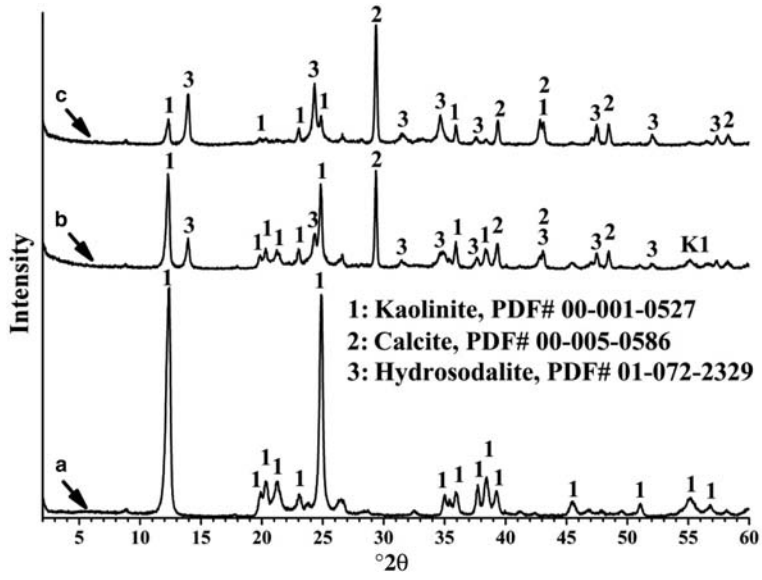

FIG. 3. XRD patterns of the: (a) SK-clay, and alkali-activated SK-clay using mass ratios of $Ca(OH)_2/Na_2CO_3$ calculated to produce NaOH with NaOH/clay mass ratios equivalent to (b) 0.16 and (c) 0.32.

https://doi.org/10.1180/claymin.2017.052.4.06 Published online by Cambridge University Press

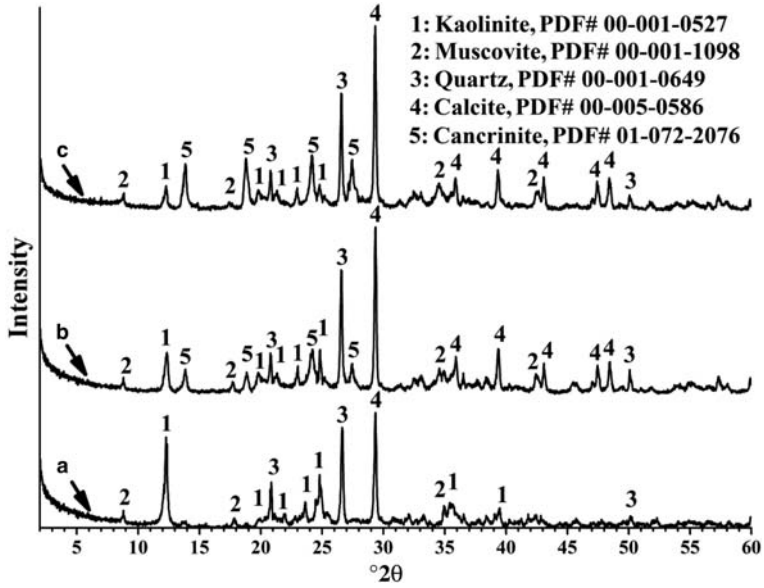

FIG. 4. XRD patterns of the: (a) JHK-clay and alkali-activated JHK-clay using mass ratios of $Ca(OH)_2/Na_2CO_3$ calculated to produce NaOH with NaOH/clay mass ratios equivalent to (b) 0.16 and (c) 0.32.

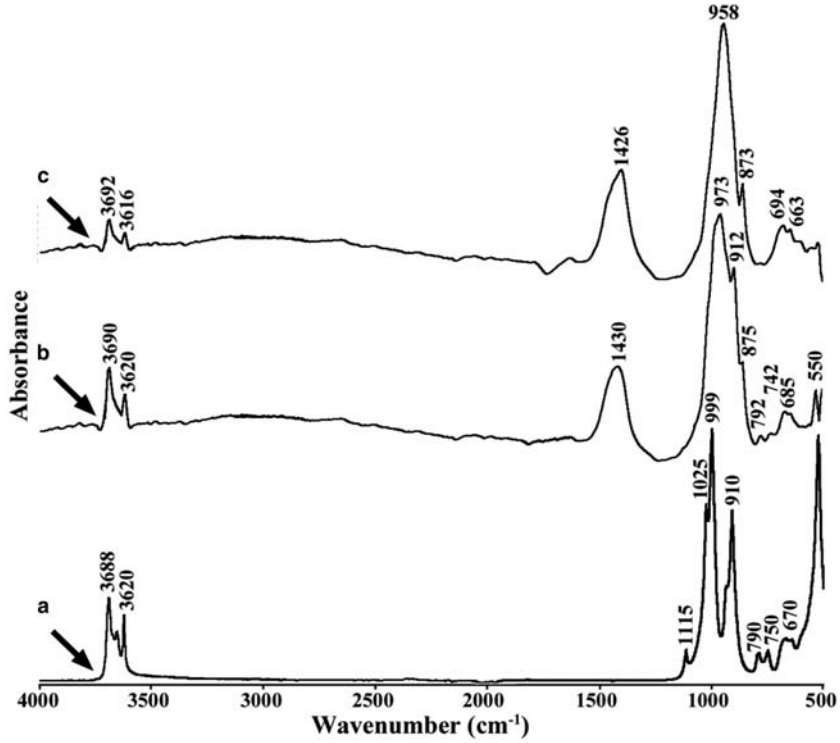

FIG. 5. ATR-IR spectra of: (a) SK-clay, SK-clay alkali-activated materials using mass ratios of $Ca(OH)_2/Na_2CO_3$ calculated to produce NaOH with NaOH/clay mass ratio equivalent to (b) 0.16 and (c) 0.32.

https://doi.org/10.1180/claymin.2017.052.4.06 Published online by Cambridge University Press

The hydrothermal synthesis of pure cancrinite without a disordered intermediate phase by reaction between kaolinite and NaOH-Na_2CO_3 occurs at temperatures below 200°C (Hackbarth *et al.*, 1999). According to Hackbarth *et al.* (1999), the NaOH-Na_2CO_3 system is also responsible for producing cancrinite by alkali-activation of JHK-clay using the $Ca(OH)_2/Na_2CO_3$ alkaline mixture. This finding suggests the possible formation of Na_2CO_3 during alkali-activation through a partial reaction between NaOH (equation 3) and the calcite originally present in the JHK-clay.

The ATR-IR spectra of the raw clays and the alkali-activated materials are shown in Figs 5 and 6. The IR spectra of raw clays (Figs 5a and 6a) exhibit three distinct regions: (1) the Al-O bending mode of AlO_6 octahedra (bands at 670, 750 and 790 cm^{-1}); (2) the asymmetric stretching mode of the Si–O–*T* (*T* = Si or Al) region (bands at 910, 999, 1025 and 1115 cm^{-1}); and (3) the stretching mode of the –O-H region (bands at 3960, 3650 and 3620 cm^{-1}). The spectra of the alkali-activation materials (Figs 5b,c and 6b,c) display a remarkable decrease in the intensity of the Al-O bending modes and stretching modes of –O-H region, with increase in $Ca(OH)_2/Na_2CO_3$ mass ratios. This decrease in band intensity indicates the dissolution of kaolinite. The formation of hydroxysodalite and cancrinite was accompanied by the emergence of a single asymmetric stretching band (Si-O-T) at 958 and 962 cm^{-1}, respectively. New asymmetric stretching bands of CO_3^{2-} ions were observed at 873 and 1430 cm^{-1} assigned to $CaCO_3$, which was liberated from the $Ca(OH)_2/Na_2CO_3$ alkaline mixture.

The derivative thermogravimetric (DTG) curves of the alkali-activation products of the SK-clay and JHK-clay are shown in Figs 7 and 8, respectively. The thermal decomposition of the alkali-activated materials takes place in three decomposition steps. Step I is reflected by a broad endothermic peak in the range 40–300°C. The mass-loss values of this phase increased with increase in the mass ratios of alkaline reactant as more hydroxysodalite was produced. This is attributed to desorption of loosely bound "zeolitic" water (Knowlton *et al.,* 1981). Step II is reflected by a broad endothermic peak between 300 and 600°C. The step II thermal events are attributed to the desorption of tightly bound "zeolite" water (Vučelić *et al.,* 1973;

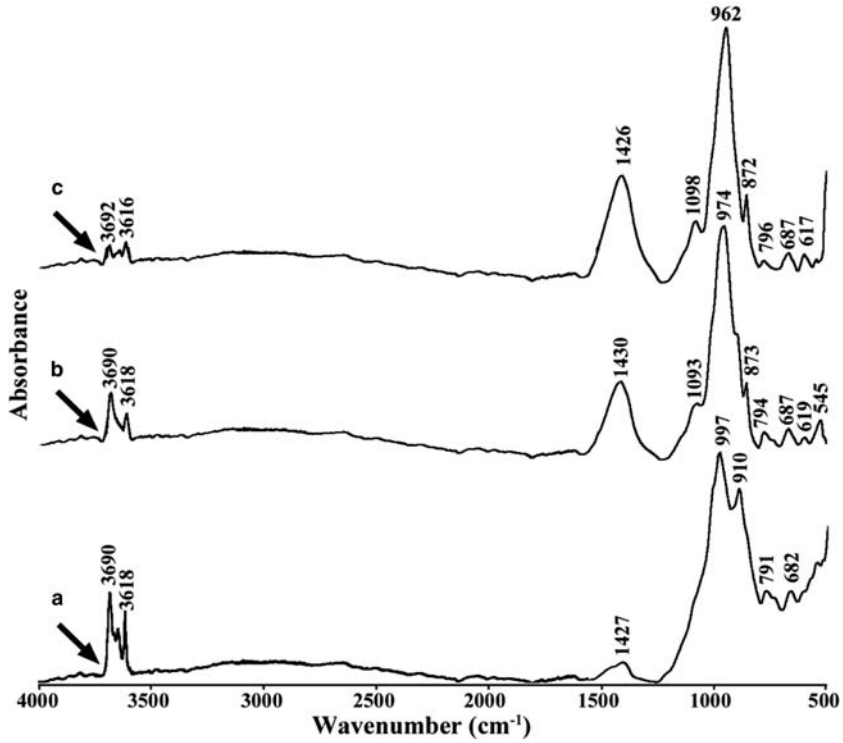

FIG. 6. ATR-IR spectra of: (a) JHK-clay, JHK-clay alkali-activated materials using mass ratios of $Ca(OH)_2/Na_2CO_3$ calculated to produce NaOH with NaOH/clay mass ratio equivalent to (b) 0.16 and (c) 0.32.

https://doi.org/10.1180/claymin.2017.052.4.06 Published online by Cambridge University Press

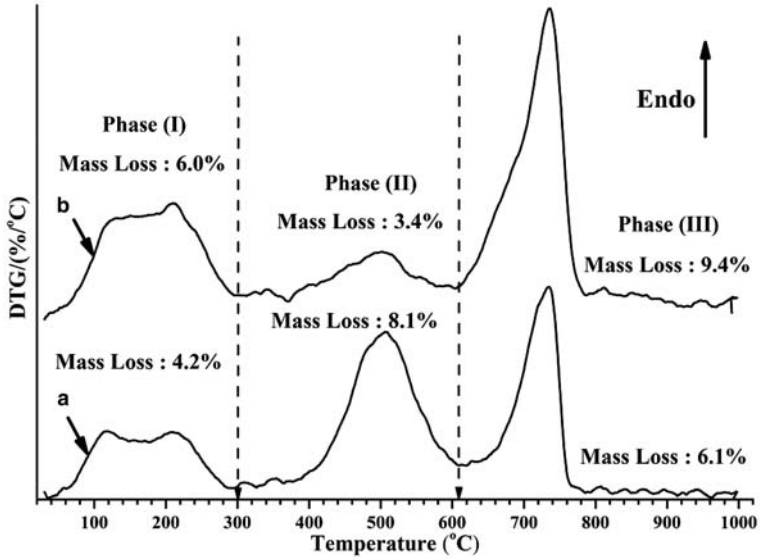

FIG. 7. DTG curves of SK-clay alkali-activated materials using mass ratios of $Ca(OH)_2/Na_2CO_3$ calculated to produce NaOH with NaOH/clay mass ratio equivalent to (a) 0.16 and (b) 0.32.

Knowlton *et al.*, 1981; Esaifan *et al.,* 2017), and dehydroxylation of the residual kaolinite. Step III is reflected by a broad endothermic peak beginning at 500°C, with a maximum at ~700–730°C. According to the XRD results, the last endothermic phase is attributed to the decomposition of $CaCO_3$. Increasing of the mass ratios of $Ca(OH)_2/Na_2CO_3$ led to a remarkable decrease in mass loss-percentage and corresponded to the dehydroxylation of kaolinite (step II) and an increase in the mass loss corresponding to the decomposition of $CaCO_3$ (step III). This finding suggests a greater reaction extent between $Ca(OH)_2$

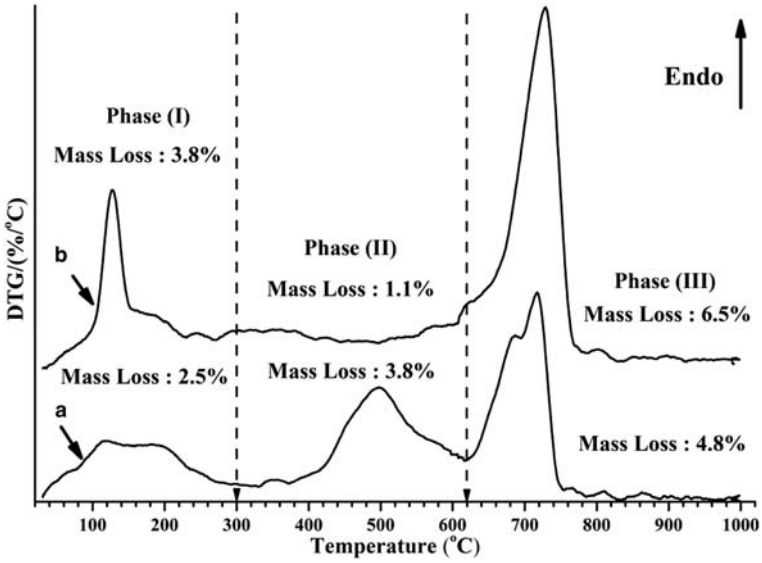

FIG. 8. DTG curves of JHK-clay alkali-activated materials using mass ratios of $Ca(OH)_2/Na_2CO_3$ calculated to produce NaOH with NaOH/clay mass ratio equivalent to (a) 0.16 and (b) 0.32.

https://doi.org/10.1180/claymin.2017.052.4.06 Published online by Cambridge University Press

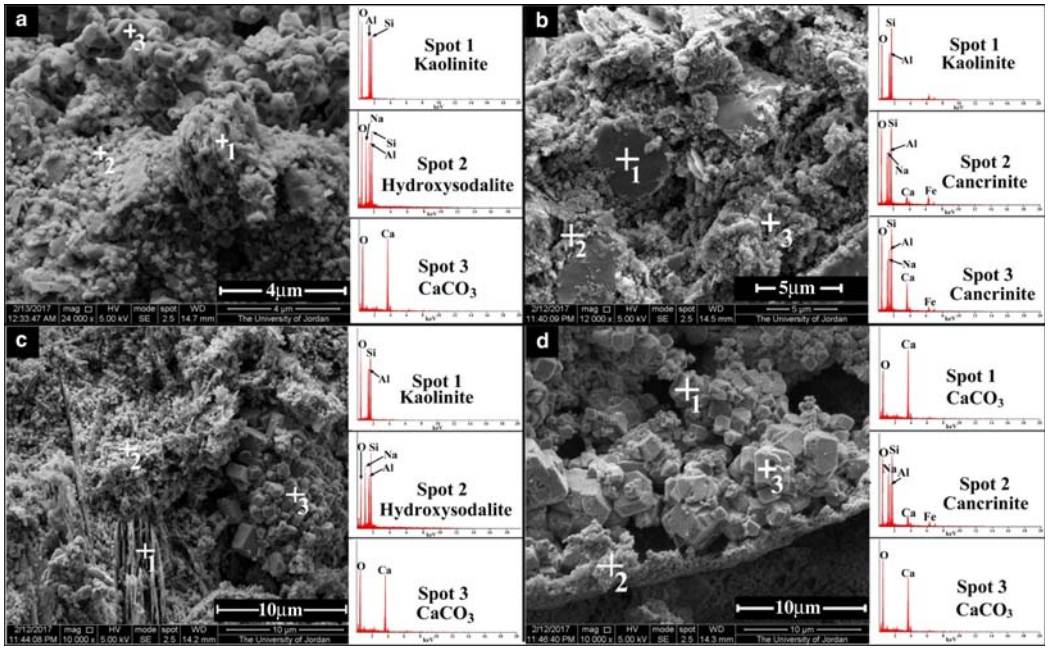

FIG. 9. SEM images of alkali-activated materials using mass ratios of $Ca(OH)_2/Na_2CO_3$ calculated to produce NaOH with mass ratio equivalent to (a) NaOH/SK-clay = 0.16, (b) NaOH/SK-clay = 0.32, (c) NaOH/JHK-clay = 0.16 and (d) NaOH/JHK-clay = 0.32.

and Na_2CO_3, which in its turn produced more NaOH and $CaCO_3$, and as a result greater consumption of kaolinite.

The SEM images of the alkali-activation products of the SK-clay and the JHK-clay (Fig. 9) are in agreement with the XRD results. The SEM/EDS micrographs of SK-clay activated material (Fig. 9a,b) confirm the formation of crystalline sub-spherical particles of hydroxysodalite which act as binding agents between residual, partially dissolved kaolinite and calcite. In the JHK-clay alkali-activated material (Fig. 9c,d), the binding phase produced was identified, based on the XRD and EDS results, as cancrinite with low Fe content which was released from the JHK-clay.

Mechanical strength and dimensional stability of the $Ca(OH)_2/Na_2CO_3$-based alkali-activated material

The unconfined strength results of the JHK-clay alkali-activated specimens prepared using NaOH solution (reference alkaline solution) and $Ca(OH)_2/Na_2CO_3$ alkaline mixture are shown in Fig. 10. The specimen strength in both alkaline activating systems increased exponentially with increasing activator concentration up to 0.16, after which only marginal strength gains occurred at a mass ratio of 0.18. Therefore, the concentration at a mass ratio of 0.16 is considered to be the economically optimum value. A maximum dry strength of 32–35 MPa was obtained for specimens prepared using NaOH solution (Fig. 10a), whereas a maximum strength of 22 MPa was obtained using $Ca(OH)_2/Na_2CO_3$ as the alkaline activating system (Fig. 10b). Although the strength values obtained by the $Ca(OH)_2/Na_2CO_3$ alkaline mixture are lower than those obtained by NaOH solution, the final strength is still within the normal range for building materials (ASTM C150/C150M-17, 2017). This variation of the strength values between the two alkaline activating systems is not yet understood though it can be explained by either or both of two reasons: (1) involvement of calcite and Na_2CO_3 (equations 3, 4) in the alkali-activated process when the $Ca(OH)_2/Na_2CO_3$ alkaline mixture was used; and (2) the chemical composition and possible variation in the binding characteristics of the alkali-activated material synthesized whether it is hydroxysodalite or cancrinite carbonate. Further investigation will be carried out in the second stage of the research project to explore the dissolution of

https://doi.org/10.1180/claymin.2017.052.4.06 Published online by Cambridge University Press

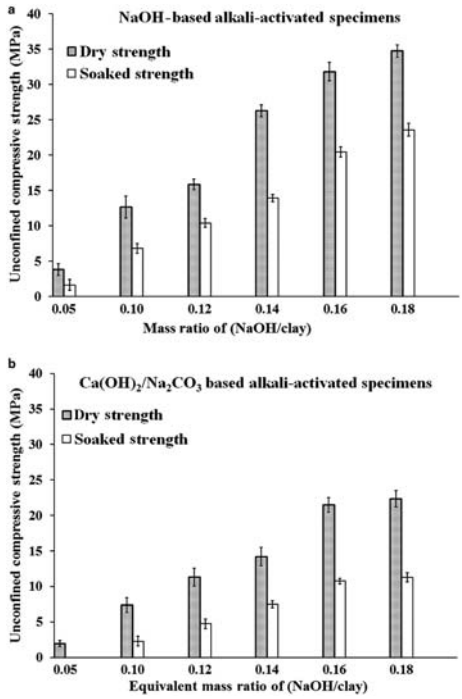

FIG. 10. Strength of dry and soaked JHK-clay alkali-activated specimens produced using: (a) an NaOH solution and (b) a $Ca(OH)_2/Na_2CO_3$ alkaline mixture.

$Ca(OH)_2/Na_2CO_3$-based alkali-activated material in aqueous solutions.

The durability of the alkali-activated specimens prepared was tested by soaking the specimens in water for 24 h, then draining them and testing for unconfined compressive strength (indicated as soaked strength). In general, a remarkable decrease in the strength was observed in comparison with the dry strength values for both alkaline activating systems. In the specimens prepared using the $Ca(OH)_2/Na_2CO_3$ alkaline mixture, the strength values observed dropped from 21 MPa to 11 MPa, and in the specimens prepared with the reference alkaline solution they reduced from 34 MPa to 22 MPa. This reduction can be explained by the presence of calcite in the final specimens' matrix which could absorb water and contribute to weakening of soaked specimens. Detailed analyses and measurements of the micro-petrophysical and mechanical characteristics of the soaked specimens will be carried out in the second stage of this research in order to fully understand the reasons for the reduction in strength upon soaking.

CONCLUSIONS

Alkali activation of kaolinite was achieved successfully with a low-cost and less chemically aggressive alkaline mixture prepared from $Ca(OH)_2$ and Na_2CO_3. The $Ca(OH)_2/Na_2CO_3$-based alkali-activated materials displayed strength values within an acceptable range for building materials (22 MPa). The reaction between $Ca(OH)_2$ and Na_2CO_3 was followed by a consecutive reaction between the NaOH produced and $CaCO_3$ which formed secondary products identified as $Ca(OH)_2$, Na_2CO_3 and pirssonite ($Na_2Ca(CO_3)_2{\cdot}2H_2O$). In the presence of kaolinite, the consecutive reaction was limited by an immediate dissolution reaction between kaolinite and NaOH to form free species of Al and Si. After curing at 70°C for 1 day, the free species crystallized into a hydrated Na-aluminosilicate phase identified as hydroxysodalite. The alkali activation of kaolinitic clay-containing calcite resulted in the production of cancrinite that acted as a binding agent.

ACKNOWLEDGEMENTS

The financial support provided by The University of Jordan under grant number 106 is greatly appreciated. The assistance provided by technical staff of the Materials Laboratory during the experimental phase of this research is acknowledged gratefully. The valuable review provided by Dr Susan White of La Trobe University, Australia, is acknowledged.

REFERENCES

ASTM C150/C150M-17 (2017) *Standard Specification for Portland Cement*. ASTM International, West Conshohocken, Pennsylvania, USA. doi:10.1520/C0150_C0150M-17.

ASTM D4318-10 (2017) *Standard Test Methods for Liquid Limit, Plastic Limit, and Plasticity Index of Soils*. ASTM International, West Conshohocken, Pennsylvania, USA. doi:10.1520/D4318-17.

Belviso C., Giannossa L.C., Huertas F.J., Lettino A., Mangone A. & Fiore S. (2015) Synthesis of zeolites at low temperatures in fly ash-kaolinite mixtures. *Microporous and Mesoporous Materials*, **212**, 35–47.

Billingham J., Breen C. & Yarwood J. (1996) In situ determination of Brønsted/Lewis acidity on cation-exchanged clay mineral surfaces by ATR-IR. *Clay Minerals*, **31**, 513–522.

Boettcher M.E. & Gehlken P.L. (1996) Dehydration of natural gaylussite ($Na_2Ca(CO_3)_2{\cdot}5H_2O$) and pirssonite ($Na_2Ca(CO_3)_2{\cdot}2H_2O$ as illustrated by FTIR

https://doi.org/10.1180/claymin.2017.052.4.06 Published online by Cambridge University Press

spectroscopy. *Neues Jahrbuch für Mineralogie Monatshefte*, 73–91.

Burciaga-Díaz O. & Escalante-García J.I. (2013) Structure, mechanisms of reaction, and strength of an alkali-activated blast-furnace slag. *Journal of the American Ceramic Society*, **96**, 3939–3948.

Carvalho J., Carvalho P., Pinto T.A. & Labrincha A.J. (2008) Activation of mixture of natural clay and glass cullet rejects. *Clay Minerals*, **43**, 657–667.

Davidovits J. (1991) Geopolymers-inorganic polymeric new materials. *Journal of Thermal Analysis Calorimetry*, **37**, 1633–1656.

Esaifan M., Rahier H., Barhoum A., Khoury H., Hourani M. & Wastiels J. (2015) Development of inorganic polymer by alkali-activation of untreated kaolinitic clay: Reaction stoichiometry, strength and dimensional stability. *Construction and Building Materials*, **91**, 251–259.

Esaifan M., Khoury H., Aldabsheh I., Rahier H., Hourani M. & Wastiels J. (2016) Hydrated lime/potassium carbonates as alkaline activating mixture to produce kaolinitic clay based inorganic polymer. *Applied Clay Science*, **126**, 278–286.

Esaifan M., Hourani M., Khoury H., Rahier H. & Wastiels J. (2017) Synthesis of hydroxysodalite zeolite by alkali-activation of basalt powder rich in calc-plagioclase. *Advanced Powder Technology*, **28**, 473–480.

Gavryushkin P.N., Thomas V.G., Bolotina N.B., Bakakin V.V., Golovin A.V., Seryotkin Y.V. & Litasov K.D. (2016) Hydrothermal synthesis and structure solution of $Na_2Ca(CO_3)_2$: "synthetic analogue" of mineral nyerereite. *Crystal Growth & Design*, **16**, 1893–1902.

Gogo J. (1990) *Geological and Geotechnical Evaluation of Latosols from Ghana, and their Improvement for Construction*. Doctoral Thesis, Vrije Universiteit Brussel.

Hackbarth K., Gesing T.M., Fechtelkord M., Stief F. & Buhl J.C. (1999) Synthesis and crystal structure of carbonate cancrinite $Na_8[AlSiO_4]_6CO_3(H_2O)_{3.4}$, grown under low-temperature hydrothermal conditions. *Microporous and Mesoporous Materials*, **30**, 347–358.

Hassan I., Antao S.M. & Parise J.B. (2006) Cancrinite: crystal structure, phase transitions, and dehydration behavior with temperature. *American Mineralogist*, **91**, 1117–1124.

Khoury H. & El-Sakka W. (1986) Mineralogical and industrial characterization of the BatnEl-Ghoul clay deposits, southern Jordan. *Applied Clay Science*, **1**, 321–351.

Knowlton G.D., White T.R. & McKague H.L. (1981) Thermal study of types of water associated with clinoptilolite. *Clays and Clay Minerals*, **29**, 403–411.

Maia B.A., Neves F.R., Angélica S.R. & Pöllmann H. (2015) Synthesis of sodalite from Brazilian kaolin wastes. *Clay Minerals*, **50**, 663–675.

Menezes R.A., Paz S.P.A., Angélica RS., Neves R.F., Neumann R., Faulstich F.R.L. & Pergher S.B.C. (2017) Synthesis of ultramarine pigments from Na-A zeolite derived from kaolin waste from the Amazon. *Clay Minerals*, **52**, 83–96.

Novembre D., Di Sabatino B., Gimeno D. & Pace C. (2011) Synthesis and characterization of Na-X, Na-A and Na-P zeolites and hydroxysodalite from metakaolinite. *Clay Minerals*, **46**, 339–354.

Osornio-Rubio N.R., Torres-Ochoa J.A., Palma-Tirado M.L., Iménez-Islas H.J., Rosas-Cedillo R., Fierro-Gonzalez J.C. & Martínez-González G.M. (2016) Study of the dehydroxylation of kaolinite and alunite from a Mexican clay with DRIFTS-MS. *Clay Minerals*, **51**, 55–68. doi:10.1180/claymin.2016.051.1.05.

Pacheco-Torgal F., Castro-Gomes J. & Jalali S. (2008) Alkali-activated binders: A review: Part 1. Historical background, terminology, reaction mechanisms and hydration products. *Construction and Building Materials*, **22**, 1305–1314.

Pacheco-Torgal F., Labrincha J., Palomo A., Leonelli C. & Chindaprasirt P. (2014) *Handbook of Alkali-Activated Cements, Mortars and Concretes*. WoodHead Publishing, Cambridge, UK, pp. 56–58.

Provis J.L. & Bernal SA. (2014) Geopolymers and related alkali-activated materials. *Annual Review of Materials Research*, **44**, 299–327.

Shatskiy A., Gavryushkin P.N., Litasov K.D., Koroleva O. N., Kupriyanov I.N., Borzdov Y.M. & Ohtani E. (2015) Na-Ca carbonates synthesized under upper-mantle conditions: Raman spectroscopic and X-ray diffraction studies. *European Journal of Mineralogy*, **27**, 175–184.

Smith J.W., Johnson D.R. & Robb W.A. (1971) Thermal synthesis of sodium calcium carbonate – A potential thermal analysis standard. *Thermochimica Acta*, **2**, 305–312.

Steudel A., Mehl D. & Emmerich K. (2013) Simultaneous thermal analysis of different bentonite–sodium carbonate systems: an attempt to distinguish alkali-activated bentonites from raw materials. *Clay Minerals*, **48**, 117–128.

Van Deventer J.S.J., Provis J.L. & Duxson P. (2012) Technical and commercial progress in the adoption of geopolymer cement. *Minerals Engineering*, **29**, 89–104.

Vučelić V., Vučelić D., Karaulić D. & Šušić M. (1973) Thermal quality analysis of water on sythetic zeolite type A. *Thermochimica Acta*, **7**, 77–85.

Zhang Y.J., Zhao Y.L., Li H.H. & Xu D.L. (2008) Structure characterization of hydration products generated by alkaline activation of granulated blast furnace slag. *Journal of Materials Science*, **43**, 7141–7147.